



Nanostructured Lithium Manganese Oxide Cathodes Obtained by Reducing Lithium Permanganate with Methanol

D. Im and A. Manthiram*^z

Materials Science and Engineering Program, The University of Texas at Austin, Austin, Texas 78712, USA

Reduction of lithium permanganate with methanol in acetonitrile and acetonitrile-water media has been investigated to obtain nanocrystalline lithium manganese oxides. The products have been characterized by wet-chemical analysis, Fourier transform infrared spectroscopy, thermogravimetric analysis, X-ray diffraction, and transmission electron microscopy. The samples synthesized in acetonitrile medium consist of a considerable amount of organic residue even after firing at 250°C in vacuum, which could be lowered by introducing water into the synthesis and washing media (acetonitrile-water mixture). Additionally, introduction of lithium hydroxide into the synthesis medium helps to increase the lithium content and Li/Mn ratio in the product and thereby to improve the electrochemical performance. Optimum compositions synthesized in the acetonitrile-water medium exhibit capacities of >200 mAh/g with good cyclability and charge efficiency.

© 2002 The Electrochemical Society. [DOI: 10.1149/1.1490355] All rights reserved.

Manuscript submitted November 11, 2001; revised manuscript received February 7, 2002. Available electronically June 21, 2002.

Layered lithium cobalt oxide (LiCoO₂) is the dominant cathode material for commercial lithium-ion cells. However, its high cost has restricted the use of lithium-ion batteries to small portable electronic devices. Use of lithium-ion batteries for large high-power applications such as electric vehicles requires a considerable reduction in their cost. In this regard, manganese oxides are attractive candidates as manganese is inexpensive compared to cobalt. Additionally, manganese is environmentally benign compared to cobalt and therefore manganese oxides will be a better choice for future lithium-ion batteries as they become more broadly available.

Among the various manganese oxides, both spinel LiMn₂O₄^{1,2} and layered LiMnO₂³⁻⁵ are the most widely investigated cathodes. Unfortunately, the spinel LiMn₂O₄ exhibits limited capacity and capacity fade due to lattice distortions and manganese dissolution. On the other hand, the layered LiMnO₂ tends to transform to spinel-like phases during electrochemical cycling. As a way to circumvent some of these difficulties, amorphous or nanocrystalline manganese oxides have been pursued recently and some of them exhibit high capacity with good cyclability.⁶⁻¹⁴ It is believed that the lattice distortions caused by Jahn-Teller distortion can be accommodated more smoothly in disordered materials.¹⁰

However, the amorphous or nanocrystalline oxides are generally prepared by soft chemistry procedures and three important issues need to be considered in dealing with them: (i) the high surface area, (ii) the presence of residues that might not have been completely removed by washing, and (iii) the presence of lattice water originating from the aqueous synthesis media. The high surface area can increase the rate of unwanted reactions such as the electrolyte decomposition. The presence of residues in manganese oxides prepared by soft chemistry procedures has been noticed by several groups in the literature. For example, during the reduction of permanganate with glucose, Ching *et al.*¹⁵ proposed the formation of reaction intermediates in which MnO₄ tetrahedral units are cross-linked with organic molecules. Leroux and Nazar⁶ reported an increase in polarization with increasing amounts of the reducing agent, oxalic acid, used. Passerini *et al.*¹² reported the detection of carbon by elemental analysis in the product obtained by the reduction of lithium permanganate with lithium fumarate. Furthermore, a series of organometallic compounds reported recently show that a chemical bond between a transition metal ion and an organic molecule can be intact up to 345°C.¹⁶ Since most of the amorphous or poorly crystalline oxides for batteries are prepared under 300°C, they can be prone to the presence of organic residues.

Reduction of permanganates is a popular soft chemistry route to obtain manganese oxides.¹⁷ Various organic and inorganic reducing

agents such as oxalic acid or its lithium salt,^{6,14} lithium iodide,⁷⁻¹⁰ fumaric acid or its lithium salt,^{11-13,18,19} glucose,^{15,20} ethanol,²¹ and borohydrides²² have been investigated in this regard. Most of these reducing agents excepting lithium iodide have been invariably pursued in aqueous medium, which can lead to products containing water. The presence of water could degrade the cathode performance during long-term cycling. To overcome this difficulty, our group recently pursued the reduction of sodium permanganate with lithium iodide in acetonitrile medium.⁷⁻⁹ Although the product obtained by such a process exhibited excellent electrochemical performance, it was found to contain NaIO₃ as a byproduct.⁹

With an objective of obtaining cleaner products, we focus in this paper on the synthesis of lithium manganese oxides by a reduction of lithium permanganate with methanol and on their chemical and electrochemical characterization. By employing lithium permanganate, which has not been frequently used as a precursor for manganese oxides, we avoid the incorporation of other alkali metal ions such as Na⁺ and K⁺ into the products; the other cations could interfere with the extraction/insertion of lithium during the electrochemical charge/discharge process. Methanol was selected as a reducing agent with an aim to minimize the residue effect since methanol is one of the smallest organic molecules.

Experimental

Lithium permanganate (LiMnO₄) was supplied by Carus Chemical Company. Since LiMnO₄ is a strong oxidizer and is highly reactive, care was taken in storing and handling; it was stored in a vacuum desiccator in a small quantity. All other chemicals were reagent grade and were used without further purification. The lithium manganese oxides were synthesized by adding a predetermined quantity of methanol to a solution of lithium permanganate in either acetonitrile or a mixture of acetonitrile and water (Table I), stirring the mixture for 20 h, filtering the product, and washing it thoroughly with the solvent used for the synthesis unless otherwise specified. In some cases, lithium hydroxide was added to the lithium permanganate solution before adding methanol with an aim of increasing the lithium content in the reaction product. The lithium manganese oxides thus obtained were fired at 250°C in vacuum for 1 day and stored in a vacuum desiccator before further chemical and electrochemical characterization.

Elemental analysis was carried out with a Perkin-Elmer 1100 atomic absorption spectrophotometer (AAS). The average oxidation state of manganese was determined with a redox titration employing sodium oxalate. Fourier transform infrared (FTIR) spectra were recorded with pellets made with KBr and the sample using a Nicolet AVATAR 360 FTIR spectrometer. Thermogravimetric analysis (TGA) was carried out with a Perkin-Elmer Series 7 thermogravimetric analyzer with a heating rate of 2°C/min in flowing air (50 mL/min). The products obtained after the TGA experiments were

* Electrochemical Society Active Member.

^z E-mail: rmanth@mail.utexas.edu

Table I. Synthesis conditions and characterization data^a of lithium manganese oxides.

Sample ID	Synthesis conditions					Chemical composition				Oxidation state of Mn	Dry composition ^e	BET surface area ^f (m ² /g)	Density ^g (kg/L)
	Reactants		Solvents			Weight fractions (%)							
	LiMnO ₄ (mmol)	CH ₃ OH (mL)	LiOH (mmol)	CH ₃ CN (mL)	H ₂ O (mL)	Li	Mn	O ^c	Uncharacterized mass ^d				
A1	10	40	0	360	0	6.2	48.6	26.9	18.3	2.80	Li _{1.01} MnO _{1.90}	18.2	3.32
A2	10	40 ^b	0	360	0	3.9	31.2	18.7	N/A	3.13	Li _{0.99} MnO _{2.06}	N/A	N/A
B1	10	40	0	320	40	5.2	52.8	31.2	10.7	3.27	Li _{0.79} MnO _{2.03}	99.0	4.53
B2	10	40	0	200	160	2.4	61.9	31.4	04.3	3.19	Li _{0.30} MnO _{1.74}	121	4.40
C1	10	40	25	200	160	6.6	50.9	34.7	07.9	3.66	Li _{1.03} MnO _{2.34}	110	4.20
C2	10	40	50	200	160	8.3	47.4	33.8	10.5	3.52	Li _{1.38} MnO _{2.45}	197	3.58
C3	10	40	75	200	160	8.2	47.9	36.4	07.5	3.91	Li _{1.36} MnO _{2.61}	190	3.75
C4	10	40	100	200	160	8.0	47.5	36.6	07.8	3.86	Li _{1.33} MnO _{2.65}	219	3.51
D	10	40	50	200	160	11.00	43.3	37.2	08.5	3.97	Li _{2.00} MnO _{2.96}	174	3.53

^a Characterization data were obtained after firing at 250°C in vacuum for a day.

^b 1-Hexanol was used for this sample instead of methanol.

^c Oxygen fraction was calculated using charge neutrality principle based on the manganese content and the oxidation state of manganese.

^d Uncharacterized mass was calculated as (weight loss observed in TGA) - (weight loss corresponding to oxygen).

^e Dry composition refers to the composition without uncharacterized mass.

^f Before BET measurement, each sample was reheated at 150°C in vacuum to remove adsorbed gases.

^g Density was measured at room temperature by pycnometry with helium as filling gas.

also analyzed by AAS and titration. The chemical compositions were determined based on the wet-chemical analysis data as described elsewhere.^{6,22} Structural characterization was carried out with X-ray powder diffraction. Microstructural characterization was carried out with a JEOL 2010 transmission electron microscope (TEM). Surface area measurements were carried out with a Quantachrome Autosorb-1 Brunauer-Emmett-Teller (BET) analyzer using nitrogen gas as adsorbate. Density measurements were carried out with a Micromeritics AccuPyc 1330 pycnometer.

Electrochemical evaluation of the samples after firing in vacuum at 250°C was carried out with coin-type cells. About 120 mg of oxide sample (70 wt %) was ballmilled with conductive carbon black (25 wt %) for 10 min and then mixed with polytetrafluoroethylene (PTFE) binder (5 wt %) with a mortar and pestle. The mixture was then rolled and cut into circular cathodes of 2 cm² area. The weight of each cathode was typically around 20 mg. Coin cells were fabricated with the cathodes thus obtained, metallic lithium foil anode, and 1 M LiClO₄ in ethylene carbonate/dimethyl carbonate (1:1 v/v) as electrolyte. Cells were cycled between 1.5 and 4.0 V with a current density of 0.1 mA/cm². To compensate for the loss arising from polarization, when the charge voltage reached 4.0 V, the charging mode was changed from constant current to constant voltage and the constant-voltage mode was continued until the current became less than 0.02 mA/cm² or the charge capacity exceeded 105% of discharge capacity in order to prevent extensive overcharge.

Results and Discussion

Oxidation of alcohols with permanganates is one of the classical organic chemistry reactions. While the oxidation products of various sorts of alcohol are well characterized,²³ the reduction products of permanganate have rarely been studied before.²¹ Notwithstanding the high reactivity of permanganate, we found the actual reaction rate with methanol to be so slow that it took more than 10 h for the deep purple color of permanganate to disappear regardless of the kind of solvent used. However, the reaction was found to proceed faster in the presence of lithium hydroxide and reach completion within 10 min. The color of the as-prepared reduction product was reddish or light brown in the absence of lithium hydroxide and dark brown in the presence of lithium hydroxide.

The synthetic conditions and characterization data are summarized in Table I. The compositional analysis, surface area, and density data given in Table I were obtained after firing the reduction

products in vacuum at 250°C. Samples A1 and A2 that were obtained without any water in the reaction medium have an Li/Mn ratio of 1 as in the precursor, lithium permanganate, indicating that no lithium is lost into the filtrate or during washing; any lithium compound that might be formed as an intermediate appears to be insoluble in acetonitrile. On the other hand, samples B1 and B2 obtained in a mixture of acetonitrile and water in the absence of lithium hydroxide have an Li/Mn ratio of <1 indicating that some lithium is lost into the filtrate. However, the samples C1-C4 and D obtained in a mixture of acetonitrile and water in the presence of lithium hydroxide have an Li/Mn ratio of >1 indicating that lithium hydroxide also acts as a lithium source during synthesis.

All the samples in Table I have a significant amount of uncharacterized mass (4 to 18 wt %) apart from the Li_xMnO_z compositions that were obtained based on the manganese and lithium contents obtained from atomic absorption spectroscopy, the oxidation state of manganese before and after the TGA experiment, and the weight loss during the TGA experiment.^{6,22} In order to have a better understanding of the uncharacterized mass, the residues obtained after the TGA experiments were analyzed by FTIR spectroscopy.

Reduction in acetonitrile medium.—Figures 1 and 2 show, respectively, the TGA plots and FTIR spectra of some of the samples. The absorbance value in each IR spectrum has been normalized according to a procedure described by Potter and Rossman.²⁴ Sample A1, for example, shows no weight loss up to 300°C as it has been previously fired at 250°C in vacuum, but it exhibits a sharp weight loss at 300-470°C followed by a gradual loss above 470°C. The FTIR spectra of sample A1 (fired at $T < 500^\circ\text{C}$) show a doublet around 1500 cm⁻¹, which could be assigned to C-O stretching modes as accounted for by Barboux *et al.*²⁵ in an FTIR spectrum of an acetate precursor for lithium manganese oxides. Generally, the absorption band for the stretching of C-O single bond is found around 1200 cm⁻¹ and that for C=O double bond is found around 1700 cm⁻¹.²⁶ Therefore, one can conclude that the doublet found in between these two values around 1500 cm⁻¹ could correspond to an average C-O bond order of about 1.5. It is possible that some carboxylate groups that are coordinated to manganese like a chelate could be present. This assertion is supported by the fact that the oxidation product of methanol by permanganates in aqueous solution is formic acid (HCOOH). Since sample A1 was prepared in an

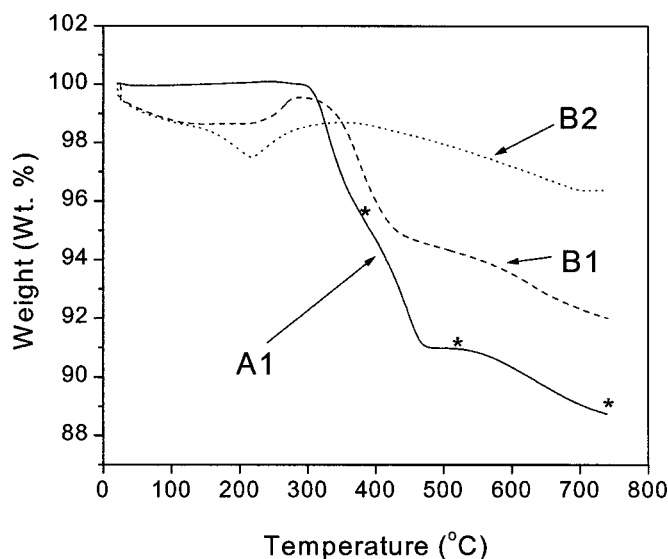


Figure 1. TGA plots of samples A1, B1, and B2 in Table I after firing at 250°C in vacuum.

aprotic solvent, manganese or lithium formate could be formed instead of its acid form. A sharp absorption band found near 860 cm^{-1} could not be assigned clearly, but it appears to be related to an organic molecule containing carboxyl group since its intensity varies according to that of the doublet at 1500 cm^{-1} .

In order to understand the reaction mechanism further, a similar reaction was carried out with 1-hexanol instead of methanol to give sample A2. Additional absorption bands near 1600 and 2900 cm^{-1}

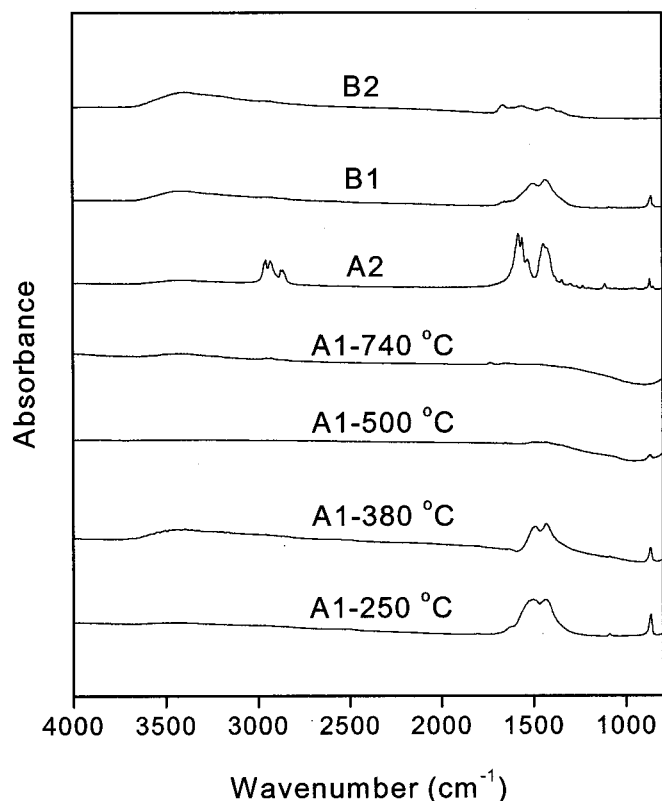


Figure 2. FTIR spectra of samples A1, A2, B1, and B2 in Table I after firing at 250°C in vacuum. For the residues obtained from TGA, the final heating temperature is indicated.

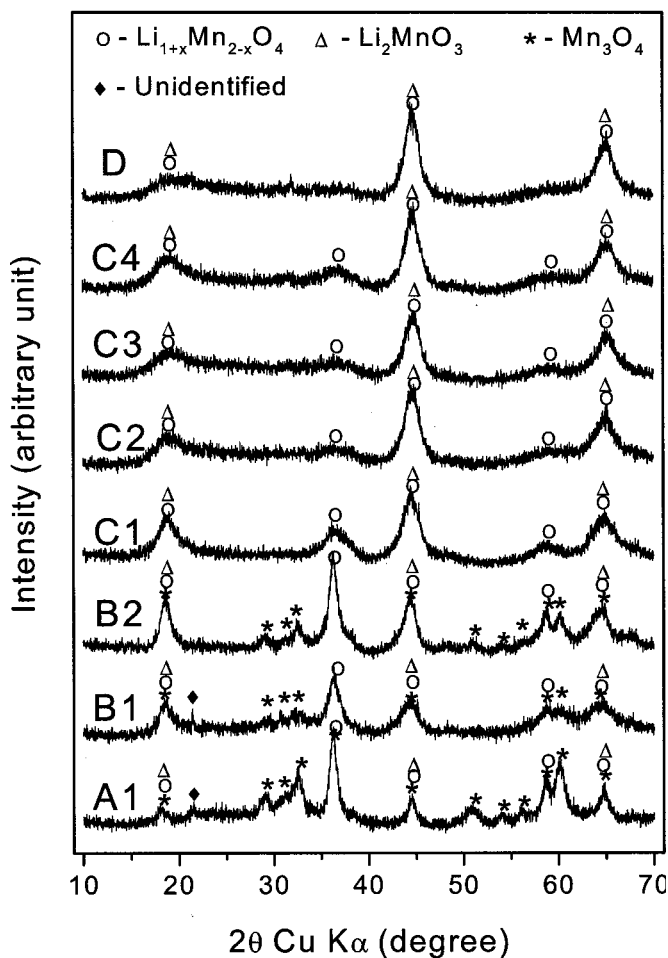


Figure 3. X-ray powder diffraction patterns of the various samples listed in Table I.

could be recognized in the spectrum of A2. The additional absorption bands indicate the presence of aliphatic hydrocarbons. Considering hexanoic acid is the oxidation product of 1-hexanol in aqueous medium, it becomes clear that the reaction mechanism in acetonitrile is similar to that in water excepting that a salt of carboxylic acid is formed in the former case instead of a free acid.

Thermal stability of the organic residue in sample A1 was assessed by recording the FTIR spectra of the residues obtained at various stages of the TGA experiment. The sampling points are 380, 500, and 740°C as marked by asterisks in the TGA plot of sample A1 (Fig. 1) and as denoted in Fig. 2. Comparison of the TGA and FTIR data confirms that the sharp weight loss starting at around 300°C is due to the decomposition of the organic species. The doublet at $\sim 1500\text{ cm}^{-1}$ and the singlet at $\sim 860\text{ cm}^{-1}$ were found to weaken gradually with increasing temperature and vanish completely at around 740°C. Surprisingly, weak absorption bands can still be seen in the sample heated up to 500°C, indicating that the carboxylates can still be present at those high temperatures. This observation suggests that even the crystalline manganese oxides prepared from acetate or similar precursors at $T < 500^\circ\text{C}$ could contain some organic residue.

Figure 3 shows the X-ray powder diffraction pattern of sample A1 after firing at 250°C in vacuum. The reflections are quite weak and broad, but the presence of crystalline phases is apparent. In addition to the obvious identification of hausmannite (Mn_3O_4), a cubic close packed spinel-like phase ($\text{Li}_{1+x}\text{Mn}_{2-x}\text{O}_4$) or Li_2MnO_3 phase is present in the X-ray pattern of sample A1. Additionally, the weak reflection present around 21° could be due to organic residue

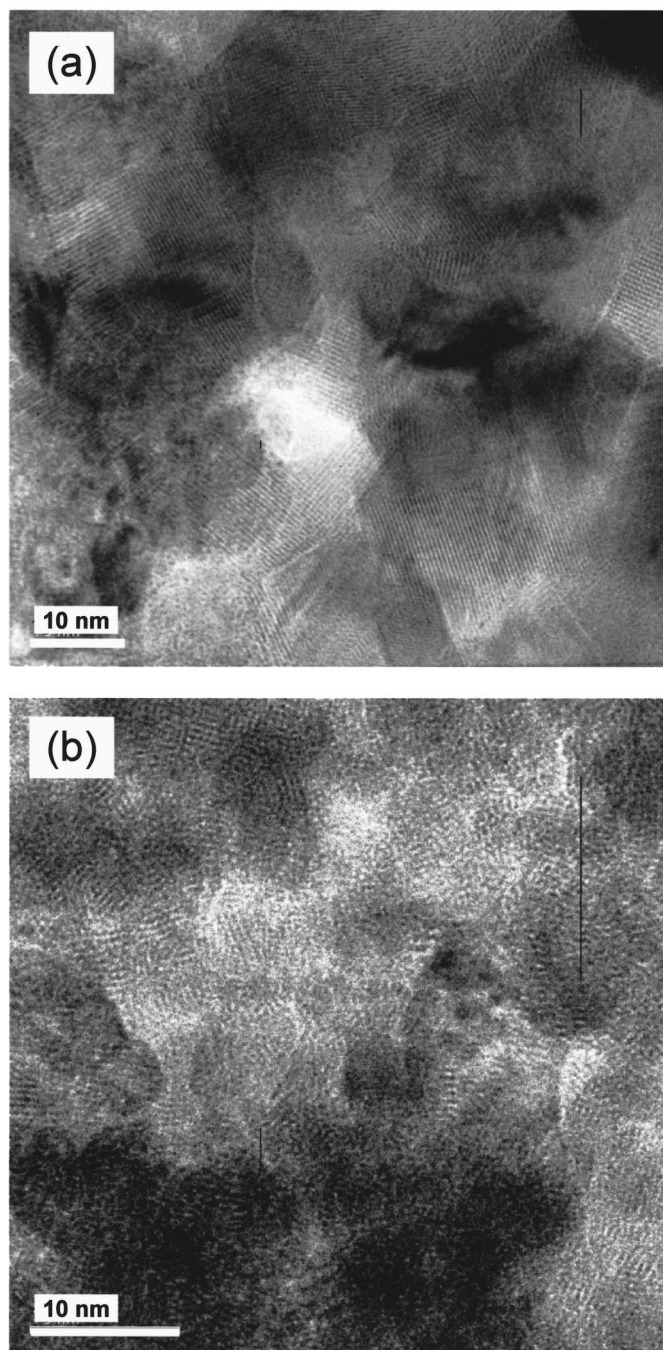


Figure 4. TEM images of (a) sample A1 and (b) sample C2.

(see later). Figure 4a shows the transmission electron microscopy (TEM) photographs of sample A1. The presence of well-developed fringe patterns confirms the nanocrystalline nature of the sample. The crystallite size was found to range from 5 to 50 nm.

The discharge voltage profile of sample A1 during its first cycle is shown in Fig. 5a. A continuous decrease in voltage from 4.0 to 1.5 V excepting a small plateau around 2.8 V suggests that the sample is predominantly composed of nanocrystalline/disordered material. Additionally, the change in slope at a few points suggests that the phase uniformity may not be good. The plateau found near 2.8 V, though representing a very small fraction of the whole capacity, is another indication of the presence of a small amount of the spinel phase. The initial capacity of about 150 mAh/g is quite low compared to that found for other amorphous manganese oxides prepared

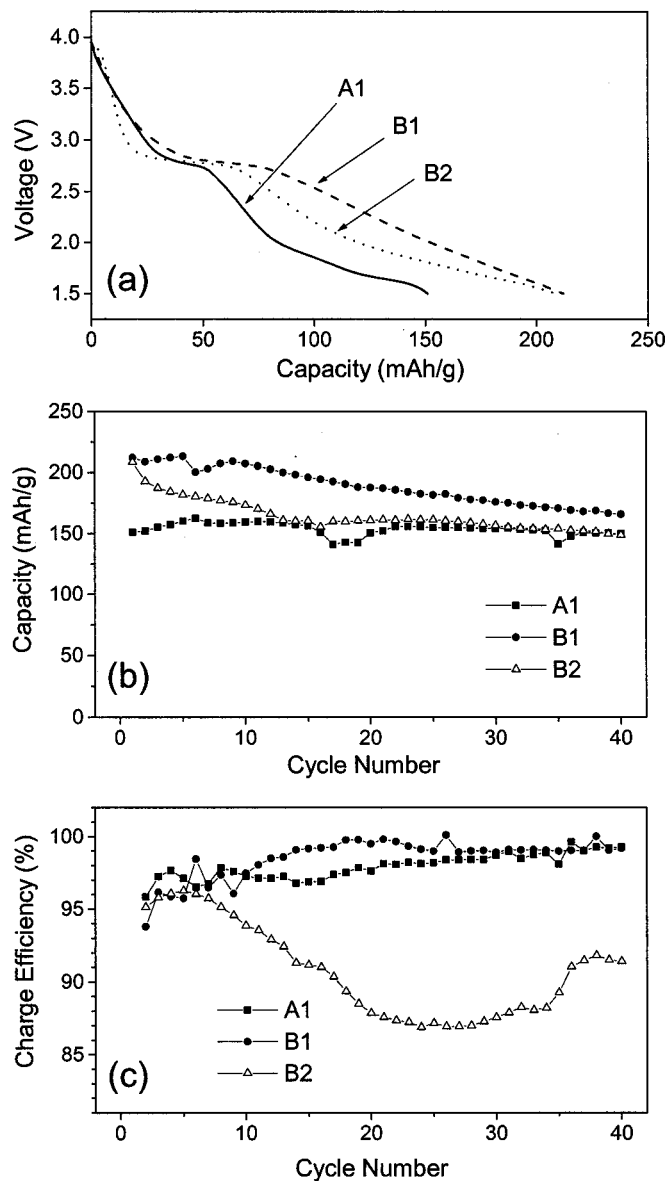


Figure 5. (a) First discharge profiles, (b) cyclability data, and (c) charge efficiency of samples A1, B1, and B2 in Table I after firing at 250°C in vacuum.

by solution-based procedures.⁷⁻¹¹ The lower capacity could be due to the presence of a significant amount of organic residue and the presence of electrochemically inactive phases such as hausmannite. Nevertheless, the sample A1 exhibits excellent capacity retention as evident from Fig. 5b. The capacity fade in 40 cycles is <1%. The charge efficiency, which is a ratio of the discharge capacity to charge capacity at each given cycle, is shown in Fig. 5c. The charge efficiency generally reflects the degree of side reactions and/or overcharge, and therefore it could represent the effect of organic residue, water, and surface area in the present set of materials. Although the charge efficiency of sample A1 is initially around 96%, it improves continuously with cycling and reaches 99% after about 30 cycles.

Reduction in acetonitrile-water medium.—Although sample A1 exhibits good cycling features, it has limited capacity and energy density due to the sloping voltage profile. With the objective for improving the capacity and energy density and for decreasing the amount of residue, we turned to pursue the synthesis in a mixed

Table II. Theoretical density of selected crystalline manganese oxides.

Formula	Mineral name or structure	Space group	Theoretical density (kg/L) ^a
MnO ₂	Pyrolusite	<i>P42/mnm</i>	5.189
MnO ₂	Ramsdellite	<i>Pnma</i>	4.826
Mn ₂ O ₃	Bixbyite	<i>Ia3</i>	5.035
Mn ₃ O ₄	Hausmannite	<i>I41/amd</i>	4.840
LiMn ₂ O ₄	Spinel	<i>Fd3m</i>	4.281
Li ₄ Mn ₅ O ₁₂	Spinel	<i>Fd3m</i>	4.056
LiMnO ₂	Layered	<i>Pm2m</i>	4.220
Li ₂ MnO ₃	Rock salt-like	<i>C2/c</i>	3.890

^a Theoretical density of each sample was calculated according to the crystallographic parameters given in JCPDS cards.

acetonitrile-water medium consisting of 10-40% water to obtain samples B1 and B2 given in Table I. The introduction of water causes significant changes in the composition of the product as seen in Table I. Both the fraction of uncharacterized mass and the lithium content (or Li/Mn ratio) decrease with increasing amount of water in the reaction medium. A decrease in both the lithium content and uncharacterized mass on going from sample A1 to samples B1 and B2 suggests that part of the lithium in the reduction product could be present as an organolithium compound, which is soluble in water but not in acetonitrile. Additionally, samples B1 and B2 prepared in the acetonitrile-water medium have higher surface areas and densities compared to sample A1 prepared in acetonitrile, possibly due to the removal of the organic residue. The densities of samples B1 and B2 are lower than those of some of the binary manganese oxides such as β -MnO₂, but higher than those of several crystalline lithium manganese oxides as seen in Table II.

The weight loss observed below 100°C in the TGA plot (Fig. 1) as well as the presence of a broad absorption band (O-H stretching vibration²⁶) between 3000 and 3500 cm⁻¹ in the FTIR spectra (Fig. 2) indicates the presence of some adsorbed water or hydroxyl groups in samples B1 and B2. Since the samples were already fired in vacuum at 250°C prior to the TGA experiment, the weight loss below 100°C indicates that these samples synthesized in acetonitrile-water medium are slightly hygroscopic. Both the samples B1 and B2 exhibit a slight weight gain around 300°C due to the incorporation of oxygen into the lattice and a weight loss above 300°C due to the decomposition of the organic residue as found in the case of sample A1. However, the weight loss occurring above 300°C decreases with increasing amount of water in the reaction medium indicating a decrease in the amount of organic residue. The decrease in the amount of organic residue is also supported by a decrease in the intensities of the absorption bands observed around 1500 cm⁻¹ (doublet) and 860 cm⁻¹ (Fig. 2). On the other hand, the intensity of the O-H stretching absorption observed around 3300 cm⁻¹ increases with increasing amount of water in the reaction medium indicating an increase in the amount of water or hydroxide in the reaction product.

The X-ray diffraction (XRD) patterns of samples B1 and B2 (Fig. 3) indicate the presence of hausmannite and a spinel-like phase as in the case of sample A1. But the amount of hausmannite appears to be more in the case of sample B2 possibly due to the lower Li/Mn ratio. Additionally, the weak reflection observed around 21° vanishes with increasing amount of water in the reaction medium confirming that this reflection is due to the organic residue as suggested earlier.

Figure 5a gives the first discharge profiles of samples B1 and B2. The discharge profiles are smoother than that of sample A1 suggesting more phase uniformity. Also, the initial discharge capacities are higher than those found for sample A1 due to the lower amount of organic residue. However, the capacity retention is inferior compared to that of sample A1 (Fig. 5b). While sample B2 exhibits poor

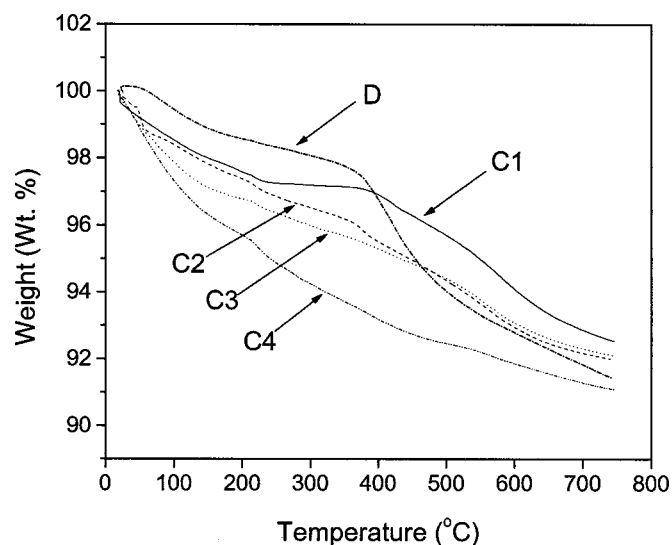


Figure 6. TGA plots of samples C1, C2, C3, C4, and D in Table I after firing at 250°C in vacuum.

charge efficiency, sample B1 exhibits good charge efficiency as sample A1 after a few cycles (Fig. 5c). The poor charge efficiency of sample B2 could be due to the presence of a higher amount of water or hydroxyl groups as they can undergo redox reactions during the charge/discharge process.

The relatively inferior cyclability of samples B1 and B2 compared to that of sample A1 could be due to the presence of water or OH groups in them. However, the capacity of sample B1 continues to fade even after the charge efficiency recovers. This observation drew our attention to another important difference between samples A1 and B1 or B2, viz. the difference in lithium content or Li/Mn ratio. Previous investigation in our laboratory of the reduction product obtained with lithium iodide has indicated an optimum Li/Mn ratio of 2 to achieve good cyclability.⁸ Accordingly, we decided to focus next on increasing the Li/Mn ratio in the reduction products obtained with methanol.

Reduction in acetonitrile-water medium in presence of LiOH.— With an objective of increasing the lithium content in the product, lithium hydroxide was incorporated into the synthesis medium (acetonitrile-water) as described in the Experimental section. The analytical data given in Table I in fact illustrate the effectiveness of this strategy in increasing the Li/Mn ratio. The Li/Mn ratio increases initially with increasing amount of lithium hydroxide, but becomes almost constant around 1.35 at higher amounts of lithium hydroxide. Additionally, the surface area and the uncharacterized mass increase while the density decreases with increasing amount of lithium hydroxide.

Figure 6 shows the TGA plots of the samples synthesized in the presence of lithium hydroxide. The continuous weight loss from ambient temperature suggests the presence of adsorbed water or hydroxyl groups. Although the samples were already fired in vacuum at 250°C prior to the TGA experiments, the weight loss occurring below 250°C suggests that these samples synthesized in a mixture of acetonitrile and water are hygroscopic unlike sample A1 (Fig. 1). Additionally, the FTIR spectra shown in Fig. 7 reveal the presence of water or hydroxyl groups as indicated by the absorption bands in the region 3000 to 3500 cm⁻¹ and carboxylate groups as indicated by the doublet around 1500 cm⁻¹.

The XRD patterns given in Fig. 3 suggest that the samples prepared in presence of lithium hydroxide consist of both Li₂MnO₃ and Li_{1+x}Mn_{2-x}O₄ where *x* is close to 0.33. The amount of Li₂MnO₃ appears to increase with increasing amount of lithium in the product. Figure 4b shows the TEM photograph of sample C2. It shows fringe patterns like sample A1 (Fig. 4a) indicating the nanocrystalline na-

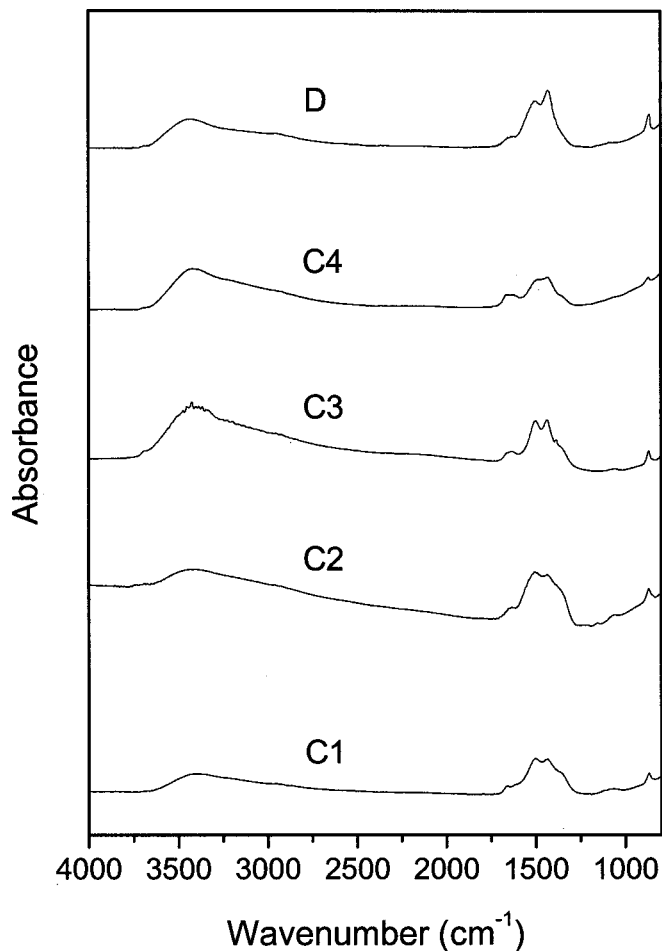


Figure 7. FTIR spectra of samples C1, C2, C3, C4, and D in Table I.

ture of the sample. However, the crystallite size was found to be much smaller (around 1 nm) than that of sample A1 (5 to 50 nm), which is consistent with the higher BET surface area of sample C2 compared to that of sample A1.

Figure 8a shows the discharge curves of the samples synthesized in the presence of lithium hydroxide. The samples show a sloping voltage profile excepting a small plateau around 2.8 V, which becomes less pronounced with increasing lithium content in the product due to the increasing amount of Li_2MnO_3 and a consequent decrease in the amount of the spinel phase. The initial capacities of these samples are higher than those of samples B1 and B2. These samples also exhibit good cyclability as seen in Fig. 8b, in which the percent capacity retention after 40 cycles for each sample is given in parenthesis. The capacity retention improves with increasing amount of lithium as anticipated in analogy with that found before for the samples obtained with lithium iodide.⁷⁻⁹

Moreover, the samples exhibit good charge efficiency (Fig. 8c) excepting sample C4, which was synthesized with the largest amount of lithium hydroxide. Interestingly, charge efficiency reaches its maximum value within a few cycles unlike the case of previous samples. The higher initial capacity, higher surface area, and faster approach to the maximum in charge efficiency suggest that the materials may have more porous structure with smaller particle size compared to the other samples as suggested by the TEM data (Fig. 4). The lower charge efficiency of sample C4 could be understood to be due to the presence of the largest amount of water or hydroxyl groups as indicated by the significantly intense O-H stretching bands ($3000\text{--}3500\text{ cm}^{-1}$) of sample C4 in Fig. 7. This explanation is consistent with the low charge efficiency of sample

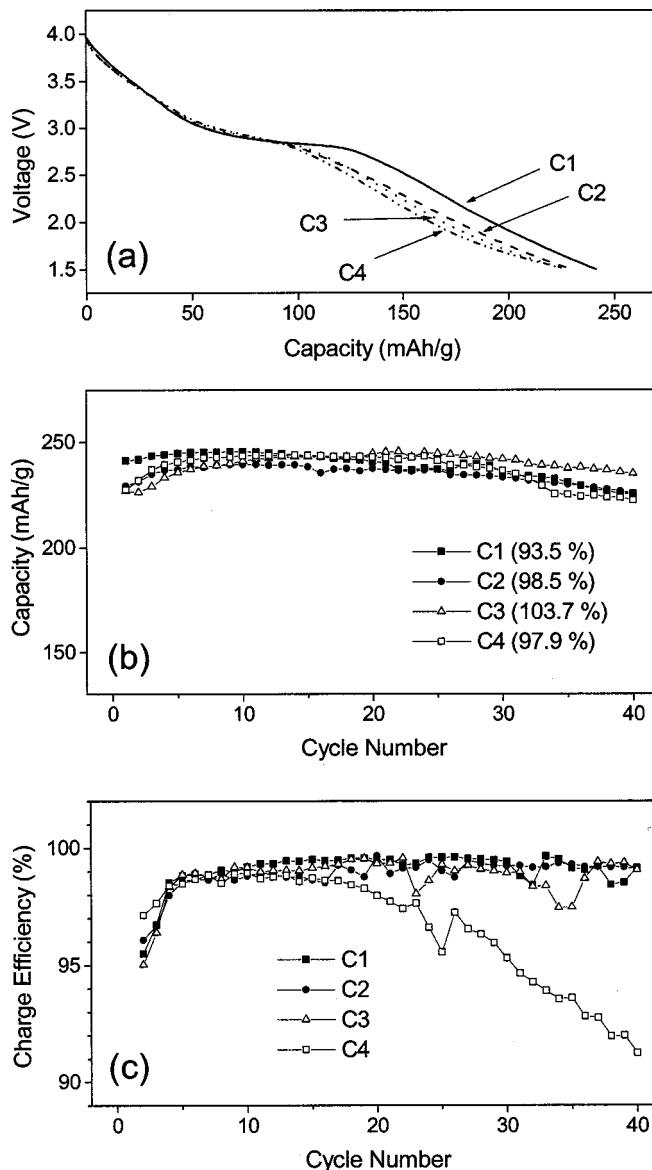


Figure 8. (a) First discharge profiles, (b) cyclability data, and (c) charge efficiency of samples C1, C2, C3, and C4 in Table I after firing at 250°C in vacuum.

B2 that also has a higher amount of water or hydroxyl group.

Encouraged by the improved performance of the samples with higher Li/Mn ratio, we pursued another strategy to increase the Li/Mn ratio further. Accordingly, sample D was prepared similarly to sample C2, but washed with only acetonitrile instead of a mixed acetonitrile-water solvent. As intended, compositional analysis shows an increased Li/Mn ratio of 2.00 in sample D (Table I). Accordingly, the XRD pattern in Fig. 3 indicates the presence of mostly Li_2MnO_3 . Also, the TGA plot is intermediate between those observed for sample A1 and the C series of samples. The discharge profile with a continuous sloping voltage (Fig. 9a) without the plateau around 2.8 V is consistent with the absence of spinel-like phase in the XRD pattern. Although the capacity is slightly lower than that of sample C2, sample D exhibits excellent cyclability with good charge efficiency (Fig. 9b and 9c).

An analysis of the characterization and electrochemical data obtained for the various samples in Table I suggests that the Li/Mn ratio is an important parameter for achieving good cyclability. Figure 10 illustrates that the capacity retention increases with increas-

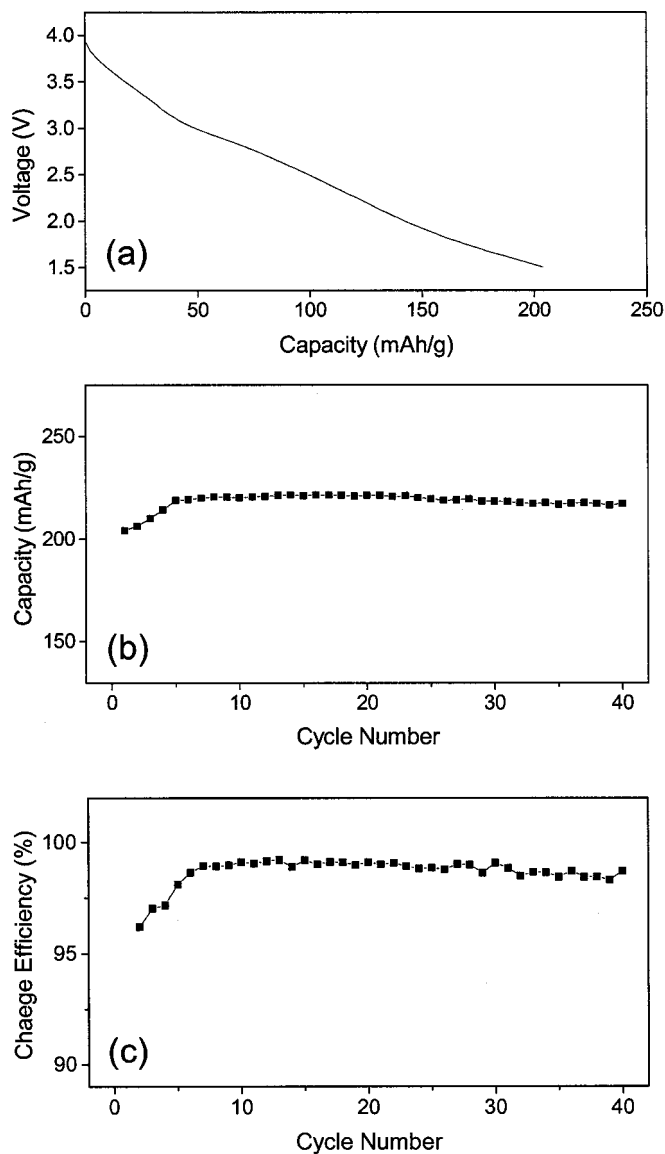


Figure 9. (a) First discharge profile, (b) cyclability data, and (c) charge efficiency of samples D in Table I after firing at 250°C in vacuum.

ing Li/Mn ratio in the product. This observation is consistent with that found for samples obtained by a reduction of sodium permanganate with lithium iodide.⁷⁻⁹ It appears that the Li/Mn ratio plays a critical role in controlling the microstructure and thereby the electrochemical performance.

Conclusions

Nanocrystalline lithium manganese oxides have been synthesized by reducing lithium permanganate with methanol in acetonitrile and acetonitrile-water media. The samples synthesized in acetonitrile medium have larger amounts of organic residue than those synthesized in acetonitrile-water medium as indicated by TGA, FTIR, and wet-chemical analysis data. The presence of organic residue leads to a lowering of capacity. The amount of residue and the sample compositions could be controlled by altering the synthesis conditions, synthesis medium (solvent), washing solutions, and incorporation of lithium hydroxide into the synthesis medium. With optimum compositions, capacities of 200-250 mAh/g with good cyclability and

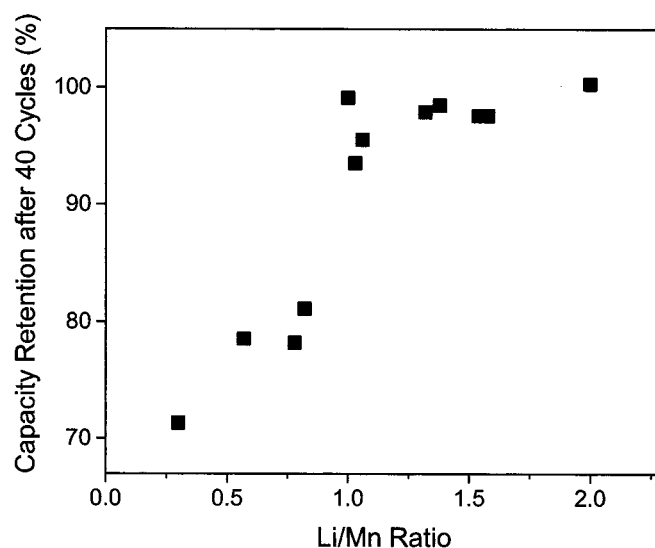


Figure 10. Relationship between capacity retention and Li/Mn ratio in the samples.

charge efficiency could be achieved. The Li/Mn ratios in the samples are found to play a critical role on the electrochemical performance of the samples as has been found before with samples obtained with lithium iodide.⁷⁻⁹

Acknowledgments

This work was supported by the NASA Glenn Research Center and Texas Advanced Technology Program Grant 003658-0488-1999. The authors thank Kil-Soo Ko for his help in TEM.

The University of Texas at Austin assisted in meeting the publication costs of this article.

References

1. M. M. Thackeray, W. I. F. David, P. G. Bruce, and J. B. Goodenough, *Mater. Res. Bull.*, **18**, 461 (1983).
2. R. J. Gummow, A. de Kock, and M. M. Thackeray, *Solid State Ionics*, **69**, 59 (1994).
3. M. M. Thackeray, *J. Electrochem. Soc.*, **142**, 2558 (1995).
4. A. R. Armstrong and P. G. Bruce, *Nature (London)*, **381**, 499 (1996).
5. F. Capitaine, P. Gravereau, and C. Delmas, *Solid State Ionics*, **89**, 197 (1996).
6. F. Leroux and L. F. Nazar, *Solid State Ionics*, **100**, 103 (1997).
7. J. Kim and A. Manthiram, *Nature (London)*, **390**, 265 (1997).
8. J. Kim and A. Manthiram, *Electrochem. Solid-State Lett.*, **2**, 55 (1999).
9. A. Manthiram, J. Kim, and S. Choi, *Mater. Res. Soc. Symp. Proc.*, **575**, 9 (2000).
10. C. R. Horne, U. Bergmann, J. Kim, K. A. Striebel, A. Manthiram, S. F. Cramer, and E. J. Cairns, *J. Electrochem. Soc.*, **147**, 395 (2000).
11. J. J. Xu, A. J. Kinsler, B. B. Owens, and W. H. Smyrl, *Electrochem. Solid-State Lett.*, **1**, 1 (1998).
12. S. Passerini, F. Coustier, M. Giorgetti, and W. H. Smyrl, *Electrochem. Solid-State Lett.*, **2**, 483 (1999).
13. B. B. Owens, S. Passerini, and W. H. Smyrl, *Electrochim. Acta*, **45**, 215 (1999).
14. A. I. Palos, M. Anne, and P. Strobel, *Solid State Ionics*, **138**, 203 (2001).
15. S. Ching, D. J. Petrovay, M. L. Jorgensen, and S. L. Suib, *Inorg. Chem.*, **36**, 883 (1997).
16. O. M. Yaghi, H. Li, and T. L. Groy, *J. Am. Chem. Soc.*, **118**, 9096 (1996).
17. S. L. Brock, N. Duan, Z. R. Tian, O. Giraldo, H. Zhou, and S. L. Suib, *Chem. Mater.*, **10**, 2619 (1998).
18. S. Bach, M. Henry, N. Baffier, and J. Livage, *J. Solid State Chem.*, **88**, 325 (1990).
19. S. Ching, J. L. Roark, N. Duan, and S. L. Suib, *Chem. Mater.*, **9**, 750 (1997).
20. S. Ching, J. A. Landrigan, M. L. Jorgensen, N. Duan, S. L. Suib, and C. L. O'Young, *Chem. Mater.*, **7**, 1604 (1995).
21. Y. Ma, J. Luo, and S. L. Suib, *Chem. Mater.*, **11**, 1972 (1999).
22. C. Tsang, J. Kim, and A. Manthiram, *J. Solid State Chem.*, **137**, 28 (1998).
23. R. J. Fessenden and J. S. Fessenden, *Organic Chemistry*, 4th ed., p. 285, Brooks/Cole Publishing, Belmont, MA (1990).
24. R. M. Potter and G. R. Rossman, *Am. Mineral.*, **64**, 1199 (1979).
25. P. Barboux, J. M. Tarascon, and F. K. Shokoohi, *J. Solid State Chem.*, **94**, 185 (1991).
26. N. B. Colthup, *J. Opt. Soc. Am.*, **40**, 397 (1950).